PROCEEDINGS OF THE ROYAL SOCIETY A MATHEMATICAL, PHYSICAL & ENGINEERING SCIENCES

The Indentation of Materials by Wedges

W. Hirst and M. G. J. W. Howse

Proc. R. Soc. Lond. A 1969 **311**, 429-444
doi: 10.1098/rspa.1969.0126

Proc. Roy. Soc. A. **311**, 429–444 (1969)
Printed in Great Britain

The indentation of materials by wedges

By W. Hirst and M. G. J. W. Howse
Department of Applied Physical Sciences, University of Reading

(*Communicated by J. Dyson, F.R.S.—Received* 4 *September* 1968)

[Plate 18]

It is shown that the mechanism and extent of the deformation of materials by wedges depends upon the angle of the indenter, and on the elasticity of the indented material as well as on its yield point. The theory for a plastic rigid solid applies only when the angle of the wedge is acute and the indented materials are of low elasticity. At more acute angles, the mechanism of deformation has been shown by Mulhearn to become one of radial compression. It is shown here that this mode of deformation is also favoured when more elastic materials are used. It is also shown that the indentation pressure approximates to that for the expansion of a semicylindrical cavity in an infinite elastic medium with definite yield point and takes the form

$$P/Y = m \ln (E/Y) + C$$

where m and C are constants, E is the Young modulus, Y the yield point in simple extension and P the flow pressure. The value of C depends upon the angle of the wedge. The result is analogous to that obtained by Marsh using a 136° pyramidal indenter, but elastic effects are more important in wedge indentation than when indenting with a pyramid. For blunt wedges and elastic materials, elastic effects predominate in importance; the process can then be regarded as that of the indentation of an ideally elastic solid by a rigid wedge. The pressure distribution on the indentation has been determined. It is shown that elastic theory satisfactorily predicts this distribution of pressure, as well as its mean value. For the indentation of highly elastic materials by acute angled wedges, the elastic and plastic deformations become comparable and the mode of deformation is very complex.

The regions of contact between solid objects deform until the contact area is sufficient to support the load between them. In two extreme situations, the deformation can be determined theoretically. Below the elastic limit the methods of classical elasticity apply, and, in contrast, when the deformations are so large that elastic deflexions become negligible, the theory for the plastic-rigid solid may be used. The intermediate region where the elastic and plastic deflexions are comparable is the least well understood. The work which has been done on the phenomena in this region has largely been stimulated by its relevance to the basic mechanisms of friction and wear, and to hardness testing.

When a hard ball is placed on a softer flat surface and an increasing load is applied, plastic flow first occurs at a point beneath the surface (see, for example, Tabor 1951). At this stage, the mean pressure under the ball is $1.1\,Y$, where Y is the elastic limit of the material of the flat, and when the load is removed the dent is broad and shallow. When the ball is pushed in further, the sides of the indentation slopes more steeply, and the mean pressure rises attaining a maximum of about $3\,Y$. When pointed indenters such as cones, pyramids, or wedges are used, the impressions made at different loads are geometrically similar; the mean pressure is independent of the size of the indentation but it varies with the apex angle. Hill, Lee

& Tupper (1947) obtained the solution for the indentation of a plastic rigid solid by a wedge. The mean indentation pressure increases with the angle of the wedge and for a semiangle of 90°, when the indenter becomes a flat punch, the indentation pressure is about 2.6 times the pressure at zero angle. It will be noted that the indentation pressure varies with the ratio of depth to breadth of the indentation in the opposite sense from before. Hill *et al.* experimented with sharp steel indenters pushed into lead, the largest semiangle employed being 30°; up to this value their theory was obeyed satisfactorily. These results have been supported by Dugdale (1953) who examined the impressions made in cold worked metals by wedge indenters having various angle.

Samuels & Mulhearn (1957) investigated the subsurface deformation associated with the indentations made in hardness testing by a pyramidal indenter. They found that the indentations appeared to be produced by a compression mechanism rather than the cutting type of Hill *et al.* Mulhearn (1959) subsequently showed that the mechanism of indentation depends on the angle of the indenter; in this later work both wedge-shaped and pyramidal indenters were used. For the indentation of a plane by a wedge, the Hill mechanism operates when the semiangle of the wedge is less than 30°. In excess of this, a different mechanism begins to operate and become increasingly important, the larger the wedge angle. At large angles, the deformation may be approximately represented as a radial compression centred at or slightly below the bottom of the indentation. Mulhearn assumed that this effect was associated with the increased importance of elastic deformation at large wedge angles; he did not measure the surface stresses.

Marsh (1964) pointed out that the Mulhearn picture of the deformation in hardness testing is analogous to the expansion of a spherical cavity by an internal pressure; the solution of this problem is known (Hill 1950). Marsh showed, moreover, that the elasticity of the deforming material is an important factor; materials with a high value of the ratio Y/E where Y is the yield stress and E the elastic modulus (i.e. highly elastic materials) would be more amenable to radial compression and the change to a radial flow mode of deformation would occur more easily. He showed that the ratio P/Y, where P is the flow pressure, would then take the form

$$P/Y = C + KB \ln Z \tag{1}$$

where C and K are constants, and B and Z are functions of Y/E. Hardness tests were made on a standard Vickers hardness machine for a diverse range of materials. For values of $B \ln Z$ less than about 4, the values of P/T obeyed equation (1), the values decreasing with increasing elasticity. For $B \ln Z > 4$, the values of P/Y were constant at about 3.2, resembling the behaviour of a plastic rigid system. (Marsh's results are shown in figure 1.)

The present work was prompted by a consideration of the physical processes in the ruling of diffraction gratings, in particular of the factors likely to influence the shape of the ruled line, the blaze angle and the wear of the ruling tool. As a simplification, the problem was regarded as the indentation of a solid by a wedge.

The values of P/Y for materials covering a range of values of the parameter Y/E has been obtained. Since the pattern of results might be expected to depend on the angle of the wedge, this effect has also been investigated. The ratio P/Y is a measure of the effective hardness of the indented material. In the ruling processes, this not only determines the width of a ruled line for a given load on the ruling tool, it also determines the pressure on the ruling tool which is causing it to wear. Attempts have also been made to determine the distribution of pressure on the indenter, the original reason being that it was thought that uniform wear of a tool would be less

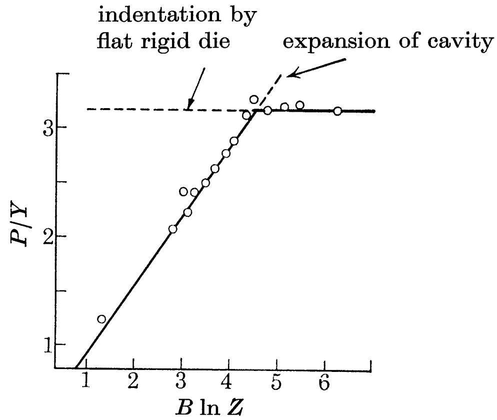

FIGURE 1. Marsh's (1964) results for P/Y for a range of materials plotted against $B \ln Z$.

disadvantageous than non-uniform wear. It was found that the pressure distributions which were obtained provided new information about the role of elastic deformation in wedge indentation. It is shown that when a range of wedge angle is employed, and materials of widely differing elasticity are indented, there are four main mechanisms of deformation. One is the mechanism for the plastic rigid solid. The second is that of radial compression, a mechanism whose nature is clarified by the present experiments, and two new mechanisms which occur when there is an appreciable degree of elastic recovery on removal of the load.

EXPERIMENTAL

(a) *Apparatus*

The apparatus was designed to ensure that the loading was uniform, and the indentation of uniform width. The load was applied through a loading arm allowing useful loads between 0.25 and 30 Kg. Indentations were made in a similar way to those in hardness tests. The indenter was gently lowered and the full load was then applied, usually for 15 s. The resulting projected area of the indentation was measured and the flow pressure, P, calculated, where

$$P = \frac{\text{load}}{\text{projected area of indentation}}$$

To test the apparatus, a Vickers diamond pyramid was substituted for one of the wedges and hardness values obtained. These agreed to within 1 % of those from a conventional Vickers hardness testing machine. The thickness of the specimen was usually about fifty times the width of the indentation.

(b) *Measurement of indentation profile*

To obtain the distribution of pressure on the wedge during indentation, it was necessary to measure the recovered indentation profile. When the slope of the groove face was small (less than 4°) a satisfactory method was to use a Michelson interferometer microscope. For intermediate slopes, the Talysurf profilometer was found to be more convenient. However, the diamond stylus of the Talysurf takes the form of a 90° pyramid. This made it impracticable to use the Talysurf for indentations whose included angle was less than about 100°. For such indentations, a composite block technique was used. This consisted of clamping two flat specimens together and indenting with the length of the wedge perpendicular to the common plane. The specimens were then separated and the indentation profile photographed.

(c) *Materials*

(1) *The wedges*

The diamond wedges were purchased from Messrs van Moppes and had angles of 60, 90, 120, 150 and 170° to within $\pm\frac{1}{2}°$. The interferometer microscope showed the sides of the indenters to be flat and smooth. The width of the blunt region at the tip of the wedge indenters was measured; it is very small in comparison with the width of the indentations.

(2) *The indented materials*

These materials are listed in table 1. Specimens were prepared in the form of cylinders. The metals were then heat-treated to ensure uniform mechanical properties. Each specimen was fully work-hardened by uniform compression in a Hounsfield 'tensometer'. It was found convenient to lubricate the platens with 'Aquadag' water soluble graphite grease when compressing the metals and with p.t.f.e.

TABLE 1

material	E	Y	E/Y	flow pressure (V.p.n.)
lead alloy	1640	1.98	828	6.25
aluminium	7030	15.3	459	51.3
copper	12650	39.8	318	128.3
mild steel	21170	79.1	268	258.9
beryllium copper	11250	109.7	102.6	289.1
p.t.f.e.	60.7	2.68	22.6	4·63
p.c.t.f.e.	119	7.76	15.3	9.94
nylon	164	12.5	13.1	15.6
Perspex	252	22.6	11.2	24.1

All values in Kg/mm². (1 Kg = 9.807 N).

sheet when compressing the plastics. The final amount of work-hardening compression varied between a natural strain of 1.1 and 1.5.

The yield stress, Y, of the fully work-hardened material is usually taken equal to the applied stress at the end of compression. However, since the final height diameter ratio of some of the cylinders was as low as 0.2, a correction was necessary to account for the friction between the platens and the specimen surface. An exact expression is not available but an approximate correction was obtained using Siebel's analysis (see, for example, Hill 1950). The value of Y obtained for the different materials are given in table 1.

The Young modulus, E, for the various plastics was obtained from graphs of deflexion against force for a clamped rod of the material, care being taken to avoid creep. The value of the Young modulus for the metals and the Poisson ratio for all the materials were obtained from published data. The values of E are given in table 1. Also given are the calculated values of E/Y and the values of the flow pressure as obtained from the measured Vickers hardness numbers.

Results

(i) *Lead*

Atkins & Tabor (1965) have shown recently that disparities between the results obtained by earlier workers on indentation using conical indenters are attributable to differences in the degree of work-hardening of the specimens used. They have shown that work-hardening exerts a very significant effect on the variation of apparent hardness with cone angle. In view of this, the specimens used in the first

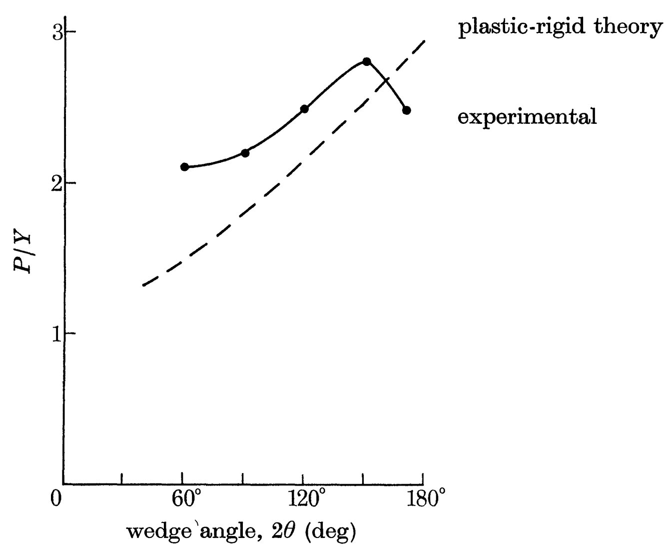

FIGURE 2. Comparison of theoretical and experimental values of P/Y for lead.

series of experiments were fully work-hardened to make them approximate as closely as possible in behaviour to a plastic-rigid solid. Figure 2 shows the variation of the mean indentation pressure with wedge angle for fully work-hardened lead. The relation predicted by Hill for the plastic rigid solid is shown for comparison. It will be observed that the experimental curve lies above the theoretical one at small wedge angles; at large angles the experimental curve falls, whereas the theoretical curve continues to rise.

The Hill theory for wedge indentation assumes that the indenter is frictionless. Grunzweig, Longman & Petch (1954) have analysed the problem allowing for friction and show that the effect is to raise the apparent indentation pressure by an amount which depends upon the angle of the wedge and the coefficient of friction.

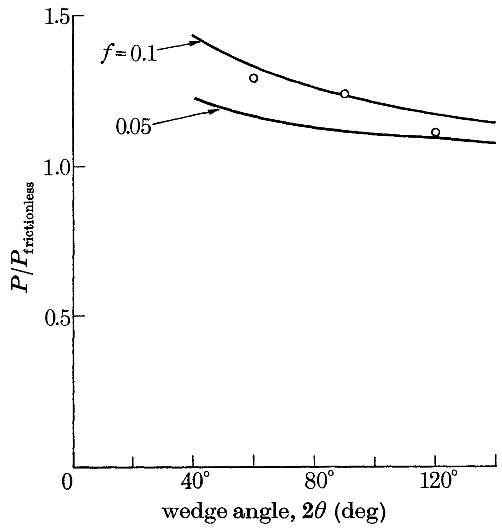

FIGURE 3. The effect of friction on the indentation pressure. ○, experimental values for lead; ——, theoretical values for a plastic-rigid material.

The friction between diamond and metals is low ($f \approx 0.05$) and, moreover, the results of figure 2 were obtained with the wedge lubricated by mineral oil. It was not therefore thought that friction would have an appreciable effect on the measured value of flow pressure. Nevertheless, in view of the disparity between the measured and theoretical values, the point was checked.

To minimize the effects due to friction, experiments were then made in which the load was applied incrementally, the diamond being raised and relubricated between successive increments, The final load was then reapplied five times, the indentation being relubricated each time. In every case examined, these 'frictionless' indentations were somewhat larger than before and the apparent flow pressures were therefore lower. The ratio of the measured flow pressure to the 'frictionless' flow pressure is plotted as a function of wedge angle in figure 3; the results as before are for lead. The figure also shows the same ratio calculated according to the theory of Grunzweig *et al.* (1954) assuming coefficients of friction of 0.05 and 0.1. It will be noted that the experimental values fall between the two theoretical curves being closer to the curve for $f = 0.1$. Similar results were obtained for aluminium.

The theoretical values of P/Y for a range of wedge angles, calculated from the theory of Grunzweig *et al.* for a coefficient of friction of $f = 0.1$, and assuming the von Mises criterion for yield ($2k = 1.15Y$ for plane strain), are shown in figure 4 as a dashed curve. For $f = 0.1$ the theoretical pressure becomes indeterminate when indenting with wedges of angle greater than about 150°. Hill (1950) has suggested that at large angles friction locks the indented material to the wedge, so that the

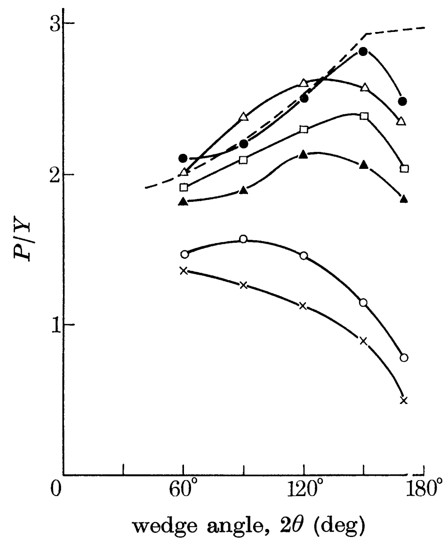

FIGURE 4. P/Y against wedge angle for different materials. △, Aluminium; ●, lead; □, copper; ▲, beryllium copper; ○, p.t.f.e.; ×, nylon; ----, plastic rigid theory with $f = 0.1$.

indenter becomes covered with a 90° wedge-shaped cap of dead material. Hill's method has been used to calculate the theoretical values of P/Y for wedges greater than 150°. It predicts a slight increase in the value of P/Y between 150° and 180°. It will be seen that the theoretical curve and the experimental results for lead agree well at angles up to 150°. At larger angles the experimental results fall appreciably below the theoretical values

(ii) *Other materials*

Indentation experiments were made using materials of differing elasticity. The values of P/Y which were obtained are also shown in figure 4; the values of E/Y range from 13 for nylon to 820 for lead. It will be seen that the more elastic the material (i.e. the smaller E/Y) the smaller is the region over which P/Y increases the angle. It therefore seems that the decrease in P/Y at the larger angles of indentation is to be attributed to elastic effects.

The expansion of a cylindrical cavity

Equation (1) was obtained by representing the deformation in hardness testing as the expansion of a hemispherical cavity. For deformation by a wedge, the analogous mode of deformation is the expansion of a cylindrical cavity in an infinite medium. Extending Hill's (1950) analysis, one obtains

$$P/Y = (1+A\ln W)/\sqrt{3} \tag{2}$$

where
$$A = \frac{2}{2-\alpha}, \quad W = \frac{2}{2\beta+\alpha-\alpha\beta}$$

$$\alpha = 3(1-2\nu)(2Y/\sqrt{3}E), \quad \beta = (1+\nu)\,2Y/\sqrt{3}E$$

and ν is the Poisson ratio.

This equation simplifies to

$$\frac{P}{Y} = \frac{1}{\sqrt{3}}\left(1+\ln\left\{\frac{\sqrt{3}}{(5-4\nu)}\frac{E}{Y}\right\}\right) \tag{3}$$

when terms involving Y^2/E^2 are neglected. For the materials used in this work the simplification does not introduce an error of more than a few parts per cent.

If the indentation of a wedge can be likened to the expansion of a cylindrical cavity, the experimental points would be expected to fall on the line

$$P/Y = m\ln(E/Y)+C$$

where m and C are constants which will be different from those inequation (3) because the expansion will be less constrained.

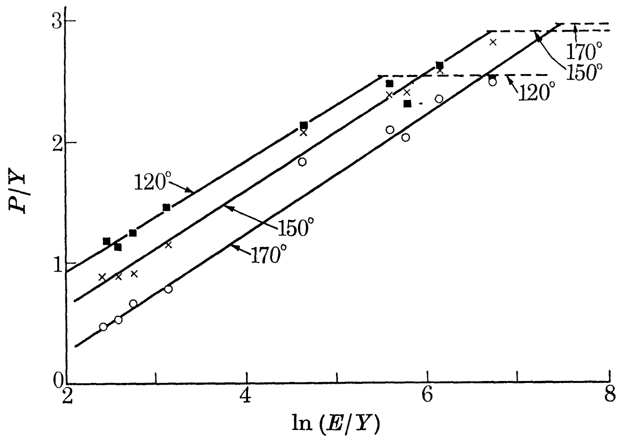

FIGURE 5. Values of P/Y for different materials plotted against ln (E/Y). ○, 170° wedge; ×, 150° wedge; ■, 120° wedge; ——, best-fit line through experimental points; – – – –, value given by plastic-rigid theory $f = 0.1$.

In figure 5 the experimental values of P/Y are plotted against $\ln(E/Y)$ for wedge angles of 120, 150 and 170°. The lines are straight and of similar slope but they are displaced from each other, reaching the theoretical plastic-rigid values of P/Y at progressively higher values of E/Y. For the 120° wedge, the change in the mode of deformation occurs at a slightly higher value of E/Y than for the 136° Vickers pyramid; i.e. wedge indentation is of a more elastic character than is the indentation made by a pyramid. For the 170° wedge even lead with E/Y above above 800 appears to deform by a mechanism which is not wholly plastic. For the sharper wedges, 60, 90 and 120°, the plots of P/Y against ln E/Y are no longer parallel in the elastic zone, but converge in the direction of increasing elasticity. Table 2 gives the values of m for different wedge angle and the values of $\ln(E/Y)_I$ where the curve for the expansion mechanism intersects the curve predicted by plastic rigid theory. It will be apparent that there is a marked change of behaviour at a wedge angle of 120°.

TABLE 2

wedge angle, 2θ	m	$(\ln E/Y)_I$
170°	0.49	7.43
150°	0.48	6.73
120°	0.46	5.51
90°	0.31	5.62
60°	0.26	5.21

The stress distribution

The theories for the indentation of a plastic rigid solid by a wedge and for the expansion of a cylindrical cavity each require the distribution of pressure on the deforming solid to be uniform. It is, however, also possible to derive an analytical solution for the indentation of a semi-infinite *elastic* solid by a wedge (see, for example, Sneddon 1951). For a purely elastic indentation the stress on the wedge at a point x is given by

$$p = \frac{E\cot\theta}{\pi(1-\nu)^2}\cosh^{-1}(a/x)$$

where $2a$ is the width of the indentation, and θ is the semiangle of the wedge. It will be seen that the pressure is not uniform but rises to infinity at $x = 0$, i.e. at the apex of the wedge. The mean pressure, p_m, however, remains finite and is given by

$$p_m = \frac{E\cot\theta}{2(1-\nu^2)}$$

One would expect, *a priori*, that for indentations produced mainly by elastic processes, these expressions would represent an approximation to the truth. They would therefore be expected to hold for the more elastic solids at higher wedge angles. Thus figure 6 compares the shape of the recovered indentation with that of the loaded indentation for a block of Perspex loaded with a 150° angle wedge. It will be seen that the recovery exceeds 80 %; for an angle of 170°, recovery is substantially complete. The theoretical mean elastic pressure to cause a 170° indentation in Perspex is 13 Kg/mm^2 which is comparable with the value of 11 Kg/mm^2

measured experimentally. As would be expected, the practical effect of the theoretically infinite central stress and gradient of stress is to cause plastic flow in such a direction as to reduce the mean pressure. In the surface itself, the elastic stress away from the centre is hydrostatic (Timoshenko 1934) and the flow should be predominantly beneath the surface.

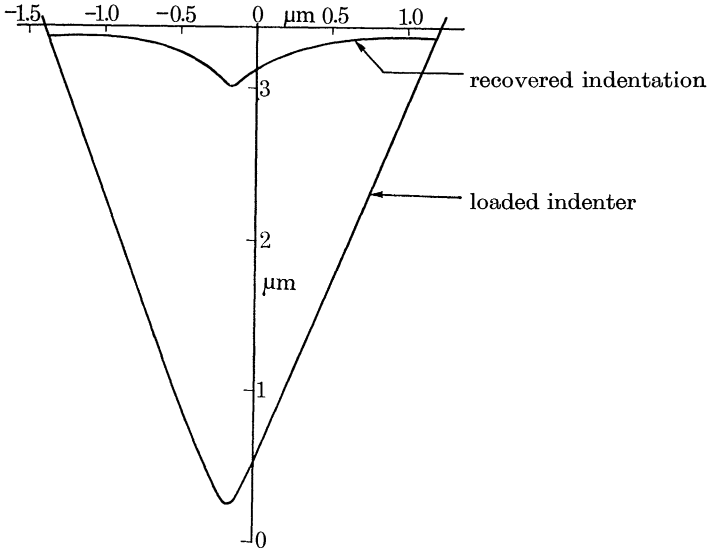

FIGURE 6. 150° wedge indentation in Perspex.

The surface depression (w) of a semi-infinite elastic solid due to a load acting uniformly along a line on the surface is given by

$$(w)_r = 2p' \frac{(1-\nu^2)}{\pi E} \ln \frac{d}{r} - \frac{(1+\nu)\,p'}{\pi E}$$

assuming plane strain (Timoshenko 1934); p' is the load per unit length of line, r is the distance from the point of application of the load and d is the depth of a point which is assumed to be fixed. With the digital computer it is then easy to derive the depression for any uniform two-dimensional system of stress by using the method of superposition. The expression to be computed is

$$w(x) = \theta \int p(\zeta) \ln |x-\zeta| \, d\zeta + k$$

where $\theta = 2(1-\nu^2)/\pi E$ and k is a constant fixed by boundary conditions. Differences between depressions do not involve k and the shape of an indentation depends only on the pressure distribution. Conversely, from the elastic deformation of the surface it is possible to calculate the stress distribution which causes the deformation; the usual method is by matric inversion for which there are standard computer programs. For a 20-point matrix, a test comparison of the numerical method with the exact values for indentation by a wedge showed that the stresses agreed, at worst, to 1 % and typically to $\frac{1}{2}$ %. This degree of accuracy was considered sufficient.

When the Perspex is under load, its surface profile is identical with the indenter. The difference between this shape and that of the recovered indentation, when the load is removed, can therefore be used to calculate the distribution of stress when the Perspex is loaded. Figure 7 shows the experimental pressure distribution derived in this way for a 170° diamond wedge. The figure also shows for comparison the theoretical distribution for purely elastic deformation together with the theoretical distribution normalized to give the same mean pressure as obtained experimentally. It will be seen that apart from a small central zone where the theoretical pressure rises towards infinity, the shape of the experimental pressure distribution resembles the theoretical one. It falls somewhat below it, and the agreement

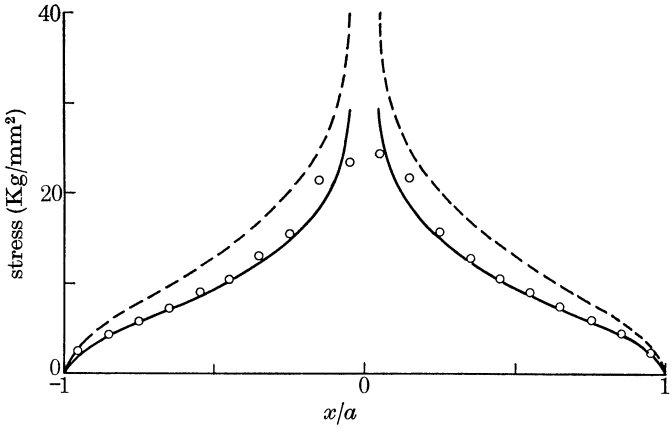

FIGURE 7. The stress distribution on a 170° diamond wedge indenting Perspex. ○, experimental values; – – – –, stress distribution for purely elastic deformation; ——, normalized elastic stress distribution.

between the experimental points and the normalized curve is excellent. Since the stress is a linear function of the depression, the effect of the plastic flow in the central zone is to produce a distribution of pressure closely resembling that for an elastic indentation by a wedge of slightly larger angle. For the 150° wedge indenting Perspex the stress distribution takes a similar form but falls further below the ideal elastic distribution; it still agrees well with the normalized elastic distribution except, as before, where the theoretical pressure rises to infinity.

At more acute angles of the wedge the central zone of high pressure, calculated from the measured surface depressions, broadens and flattens; the degree of elastic recovery diminishes and the experimental error therefore increases. For indentation of Perspex by a 120° wedge (figure 8) the experimental pressures exceed the normalized values over about half the width of the indentation. The stress distribution for a purely elastic deformation then takes values some three or four times greater than the actual stresses. For the 90° wedge and the 60° wedge the scatter in the results becomes large but there is a clear trend towards a more uniform distribution of pressure.

The stress distribution obtained when a 170° diamond wedge indents hardened tool steel (V.p.n. 860, $E/Y \simeq 50$) has also been determined. The slope of the groove face relative to the original surface recovers by about 70 % on unloading. The shape

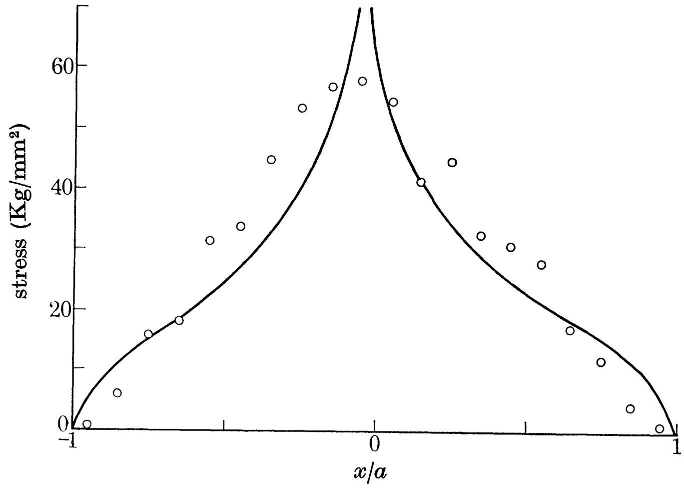

FIGURE 8. The stress distribution on a 120° wedge indenting Perspex. ○, experimental values; ——, normalized elastic stress distribution.

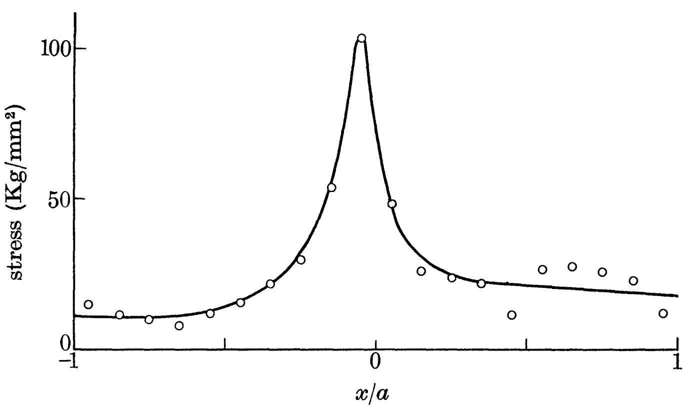

FIGURE 9. The stress distribution on a 170° wedge indenting aluminium.

of this stress distribution is similar to that for Perspex indented by a diamond wedge of angle 120°. Stress distributions have also been obtained for other metals. The distribution for a cold rolled specimen of aluminium indented by a 170° wedge is shown in figure 9; the central zone of high pressure will be observed.

The subsurface deformation

To observe the pattern of deformation beneath the surface, the composite block technique was used. Two specimens were bolted together, and indented with the length of the wedge perpendicular to the common plane. When the load was removed

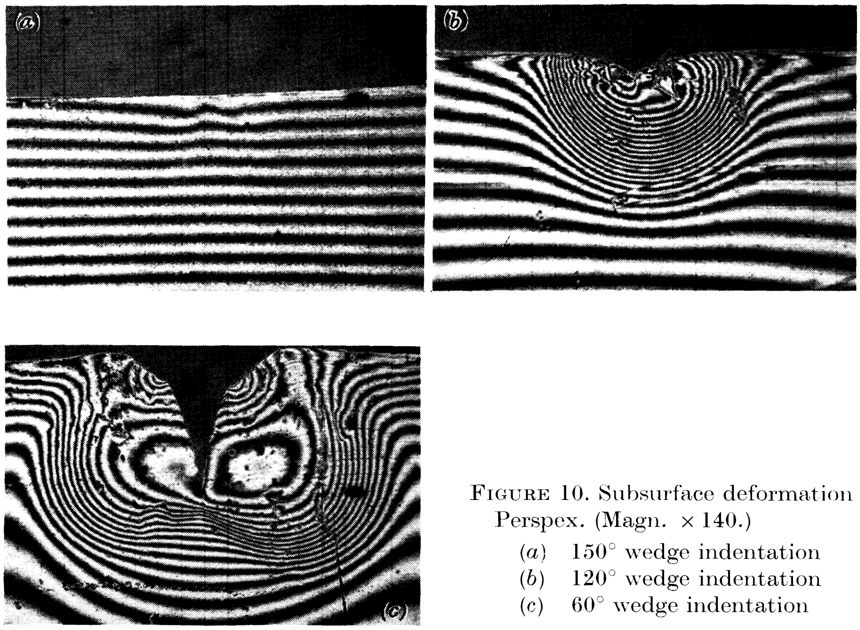

FIGURE 10. Subsurface deformation for Perspex. (Magn. × 140.)
(*a*) 150° wedge indentation
(*b*) 120° wedge indentation
(*c*) 60° wedge indentation

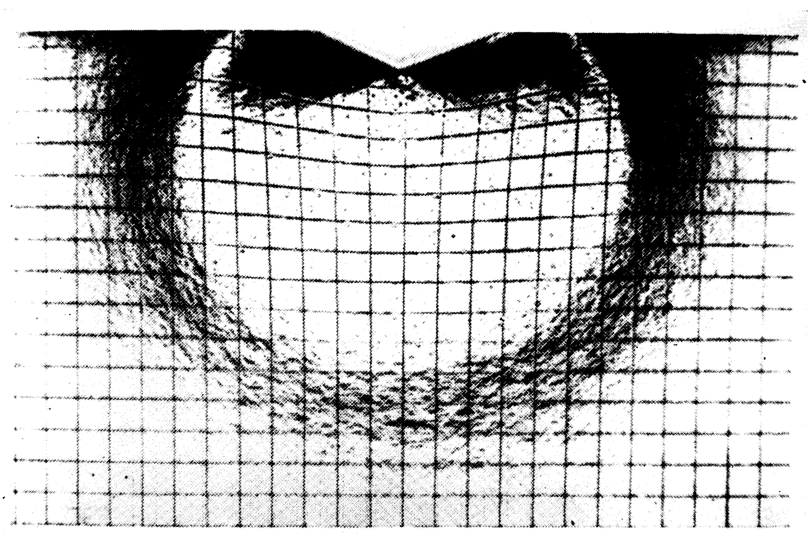

FIGURE 11. Deformation in radial compression (Mulhearn 1959).

(*Facing p.* 441)

and the specimens unbolted, the release of the residual stored stress, in a direction normal to the separated face, caused that face to bulge outwards. This strain was readily observed using a Michelson interferometer; for perspex it was convenient to deposit an evaporated film of aluminium on the surface to give better fringe contrast.

Figures 10*a*, *b* and *c*, plate 18, show the interferograms of the subsurface deformation associated with 150, 120 and 60° wedge indentations in perspex. For the 150° wedge, elastic recovery is almost complete. For the 120° wedge, the interferogram shows that close to the indentation there are similar patterns of fringes one on each side of the indentation but further away the fringes comprise a single series of concentric semicircles. For the 60° wedge the two side wings of the pattern become more pronounced, whilst further away the fringes are no longer semicircular but approximate more closely to a rectangular shape.

Discussion

These experiments show that the theory for the indentation of a plastic rigid solid by a wedge provides a satisfactory explanation of the variation of flow pressure with wedge angle only when two conditions are met. The first is that the angle of the wedge must be acute, the second that the ratio of the elastic modulus to the yield pressure of the indented material must be high. The first condition would be expected to follow from Mulhearn's discovery that when the wedge angle is increased the mode of deformation changes to one of radial compression. The second condition concerning ratio of the elastic modulus to the yield pressure relates to the degree to which a real material approximates to an ideal plastic rigid solid. The experiments show that the two conditions are inter-related so that the higher the ratio of E/Y, the greater is the range of wedge angle over which the theory for the plastic rigid solid applies.

At less acute angles, or for more elastic materials the radial mode of deformation takes over. The formulae for the variation of mean flow pressure with E/Y derived by representing the indentation process as the expansion of a cylindrical cavity in an infinite medium satisfactorily express the experimental relationships over a wide range of E/Y and of wedge angle. This two-dimensional version of Marsh's theory also shows that the results for wedges closely resemble those obtained by Marsh for a pyramidal indenter of angle 136°. The difference is that elastic effects are even more important with wedges than they are with pyramids. Thus, for equal angles of indenter, elastic effects are significant at higher values of E/Y with wedges than they are with pyramids; for an angle of 136°, the value of E/Y at the transition between elastic and plastic rigid behaviour is 200 for a pyramid, whereas the value (obtained by interpolation) for a wedge, is 500. Elastic effects are presumably more important with wedges because the stress field in a semi infinite elastic solid due to a line load varies inversely as distance whereas that due to a point load varies inversely as the square of the distance.

Figure 10*b*, showing the subsurface deformation in the so called mechanism of radial compression, makes it plain that two modes of deformation occur simultaneously. Away from the indenter, the disturbance represented by the fringes takes a cylindrical shape; in the immediate vicinity of the wedge, however, the fringe pattern subdivides showing separate wings on either flank of the indentation. The experiments have also shown that for the most obtuse angled wedges (i.e. in more elastic conditions), the distribution of surface stress is far from uniform (figure 7). Presumably this is the origin of the deformation close to the surface when conditions are more severe. The effect of the flow will be to cause the stress distribution near to the surface to become more uniform.

At large wedge angles and for highly elastic materials, the experiments make it clear that the model of an indentation as an expanding cylindrical cavity no longer applies. The main evidence is the non-uniform distribution of surface stress and the change in the pattern of subsurface damage. In this range, there is a large proportion of elastic recovery when the indenter is removed. Thus for Perspex, $E/Y \simeq 10$, the indentation made by a wedge of angle 150° recovers by some 80 % and for 170°, recovery is almost complete. In these circumstances the best model is that of the indentation of a perfectly elastic solid by a rigid wedge. This model gives a close approximation to the experimental distribution of surface stress except within a narrow central band where the pressures inevitably fall below the infinite values predicted theoretically. Even so, the central pressure remains relatively high being several times the mean pressure. For a given width of indentation, the pressures predicted for an elastic deformation increase linearly with depth. The results show that the practical effect of increasing the depth of indentation (i.e. of using sharper indenters) is to cause the mean pressure to fall further below the elastic pressure and to make the distribution of stress more uniform. Nevertheless, for blunt wedges and highly elastic materials, elastic theory provides a reasonably estimate of the mean surface pressure. For the indentation of Perspex by a wedge of angle 170°, the pressure which is predicted by elastic theory is about 15 % greater than the experimental value.

It is of interest to calculate the point at which the mean pressure for the ideally elastic model becomes equal to that for a plastic rigid solid. For the elastic solid

$$p_m = \frac{E\cot\theta}{2(1-\nu^2)}$$

For $E/Y = 200$, and $p_m/Y = 2$, $\cot I = 0.02$, or $\theta \simeq 88° 50'$, whereas for $E/Y = 10$, and $p_m/Y = 2$, $\theta \simeq 68° 12'$. It will be noted that for Perspex ($E/Y \simeq 10$), even when indented by a wedge of semiangle $\theta = 30°$, the theoretical mean stress for an ideal elastic solid is only about four times the value required by plastic rigid theory. In contrast for $E/Y = 200$, the ideal elastic stress for the same wedge angle would be ninety times the stress required by plastic rigid theory. For such materials (e.g. steel) it might therefore seem surprising that the plastic-rigid mode of deformation is delayed so long, until the angle of the wedge becomes acute.

One must, however, remember that the theoretical elastic stress and stress gradient becomes infinite at the tip of the indenter so that there will always be some relaxation of stress. For this reason a modified mode of elastic deformation might be expected to continue to smaller wedge angles than those calculated above. The question is then how far the stress can relax when the wedge angle is made steadily smaller and what will be the effect on the mode of deformation. One can set a limit to the relaxation for it clearly cannot continue beyond a state of uniform stress. The solution for the uniform loading of a portion of the surface of a semi-infinite, elastic solid is well known (Sneddon 1951). If Q is the pressure acting on the loaded zone, the shear, τ, in the material beneath the surface at a point at which the zone subtends an angle α is given by

$$\tau = -(Q/\pi)\sin\alpha$$

In this system, therefore, flow first occurs over a semicircular arc when the applied stress $Q = -\pi\,.\,k$ where k is the shear strength of the material. The resemblance of this mode of deformation to that observed by Mulhearn (1959) in the wedge (and pyramidal) indentation of metals, figure 11, plate 18, is very striking. If it be supposed that this is the operative mechanism of deformation when the elastic limit is first exceeded, the change to the behaviour of the plastic rigid solid would not then occur until the pressure appropriate to the latter model falls below πk; figure 2 shows that this takes place when the angle of the wedge is less than about 85°. Considering the crudity of the argument, this figure is in very satisfactory agreement with experiment.

This mechanism of deformation does not apply to the most elastic materials (e.g. Perspex) when the wedge angle becomes small. For these materials, there is less difference between the stresses due to plastic and to elastic strain so that there are large elastic effects even when the indenter has an angle less than 90°. Moreover, it is not to be expected that the elastically deformed zone can remain cylindrical when the indentation is deeper than it is broad. Figure 10*c*, showing the subsurface damage associated with a 60° indenter, provides experimental confirmation of this. It will also be recalled that table 2 shows that there is a marked change in the plot of P/Y against $\ln(E/Y)$ at a wedge angle of 120°. This region therefore requires yet another mode of deformation which will be of a complex elastic-plastic character.

For the indentation of real materials by hard wedges therefore four main types of deformation are observed. Figure 12 indicates the regions where they may be expected.

(1) When the angle of the wedge is very obtuse, or the material is very elastic the appropriate model is that of the indentation of an elastic solid by a wedge. This model satisfactorily predicts the shape of the distribution of surface stress except at the centre of the indentation. The mean experimental stress falls below the elastic mean stress by an amount which depends on how far the elastic limit is exceeded.

(2) For sharper wedges, producing more extensive plastic flow, the surface stress redistributes so as to become relatively uniform. There are then two zones of plastic

flow, one close to the indentation associated with this redistribution, the other further away representing the flow pattern due to the redistributed surface stress. This is the mechanism which Mulhearn has regarded as one of radial compression. It is shown in this paper that the indentation pressure approximates to that for the expansion of a semi-cylindrical cavity.

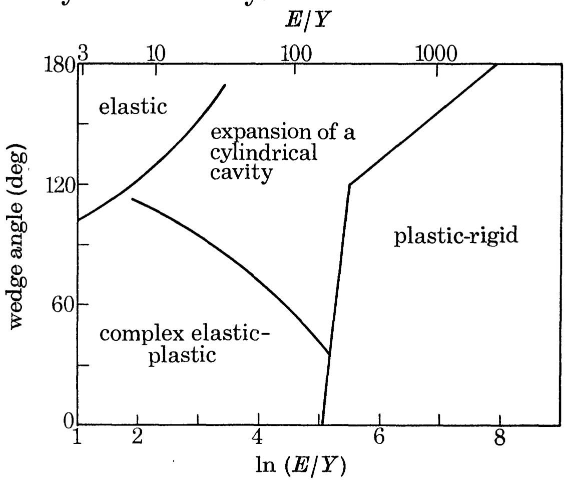

FIGURE 12. Regions of operation of the different indentation mechanisms.

(3) For acute angled wedges and materials of low elasticity, the pressure required to indent by the mechanism for a plastic rigid solid becomes less than that for mechanism (2). The theory for the plastic rigid solid then applies.

(4) For materials of very high elasticity, the wedge angle becomes acute before elastic recovery becomes negligible. The mechanism of radial compression is not observed and the deformation occurs by a complex elastic-plastic process of a kind which does not resemble any of the above types.

This work forms part of a long-term programme on the ruling of diffraction gratings initiated by the National Physical Laboratory. The authors wish to thank Dr J. Dyson, F.R.S. for many useful discussions and the N.P.L. for supporting the cost of the work and for providing a research assistantship for one of us (M.G.J.W.H.).

REFERENCES

Atkins, A. G. & Tabor, D. 1965 *J. Mech. Phys. Solids* **13**, 149.
Dugdale, D. S. 1953 *J. Mech. Phys. Solids* **2**, 14.
Grunzweig, J., Longman, I. M. & Petch, N. J. 1954 *J. Mech. Phys. Solids* **2**, 81.
Hill, R. 1950 *The mathematical theory of plasticity*. Oxford: Clarendon Press.
Hill, R., Lee, E. H. & Tupper, S. J. 1947 *Proc. Roy. Soc.* A **188**, 273.
Marsh, D. M. 1964 *Proc. Roy. Soc.* A **279**, 420.
Mulhearn, T. O. 1959 *J. Mech. Phys. Solids* **7**, 85.
Samuels, L. E. & Mulhearn, T. O. 1957 *J. Mech. .Phys. Solids* **5**, 125.
Sneddon, I. N. 1951 *Fourier Transforms*. New York: McGraw-Hill.
Tabor, D. 1951 *The hardness of metals*. Oxford: Clarendon Press.
Timoshenko, S. 1934 *Theory of elasticity*. New York: McGraw-Hill.

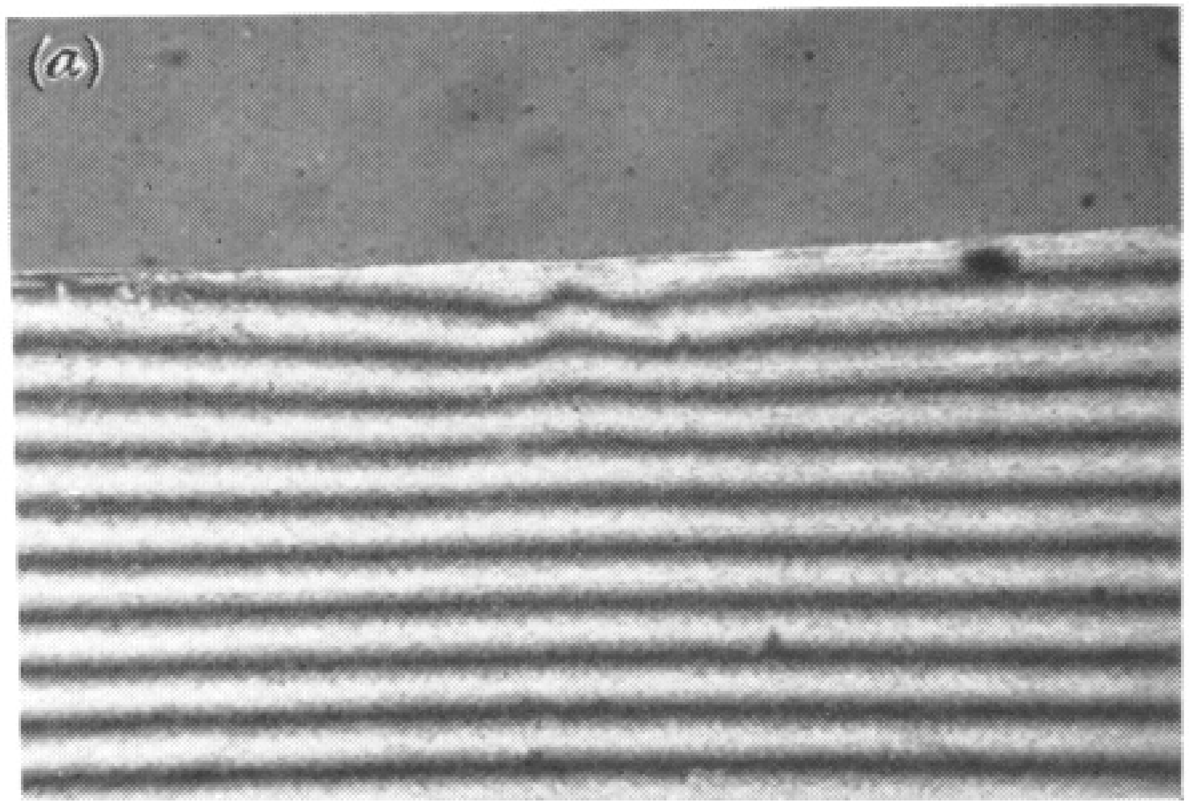

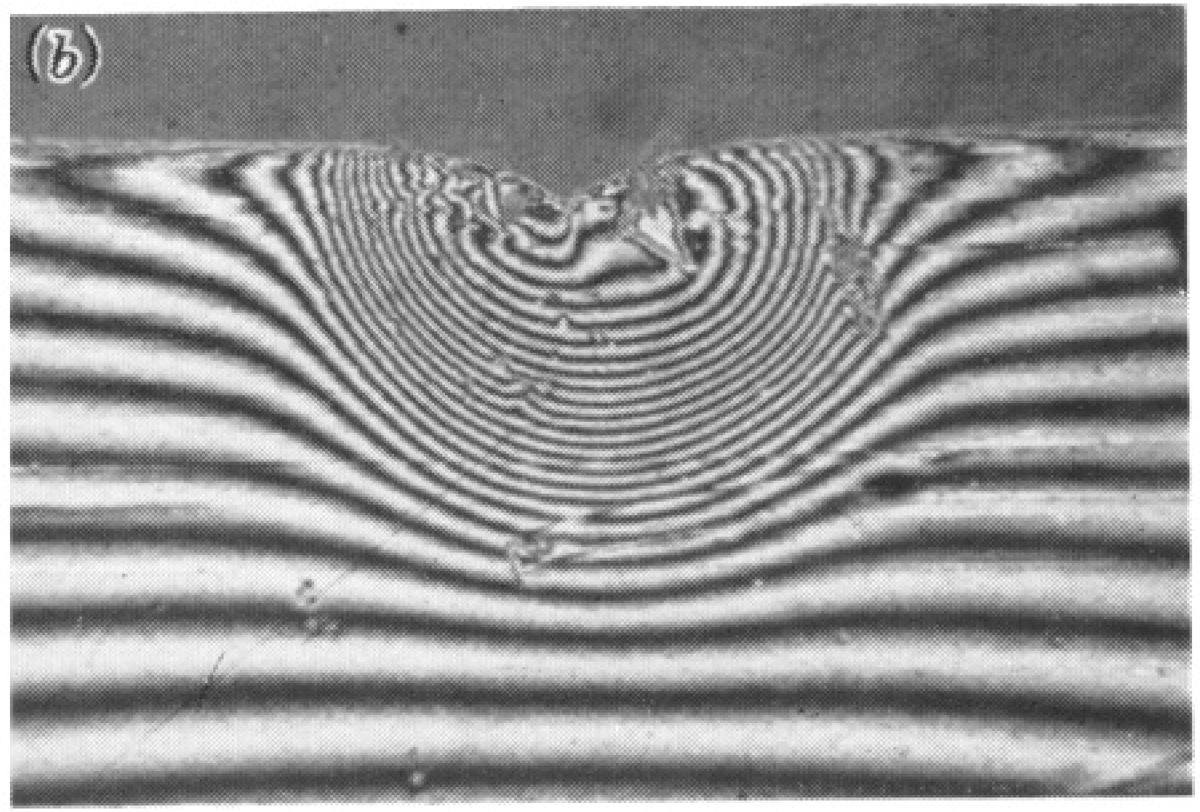

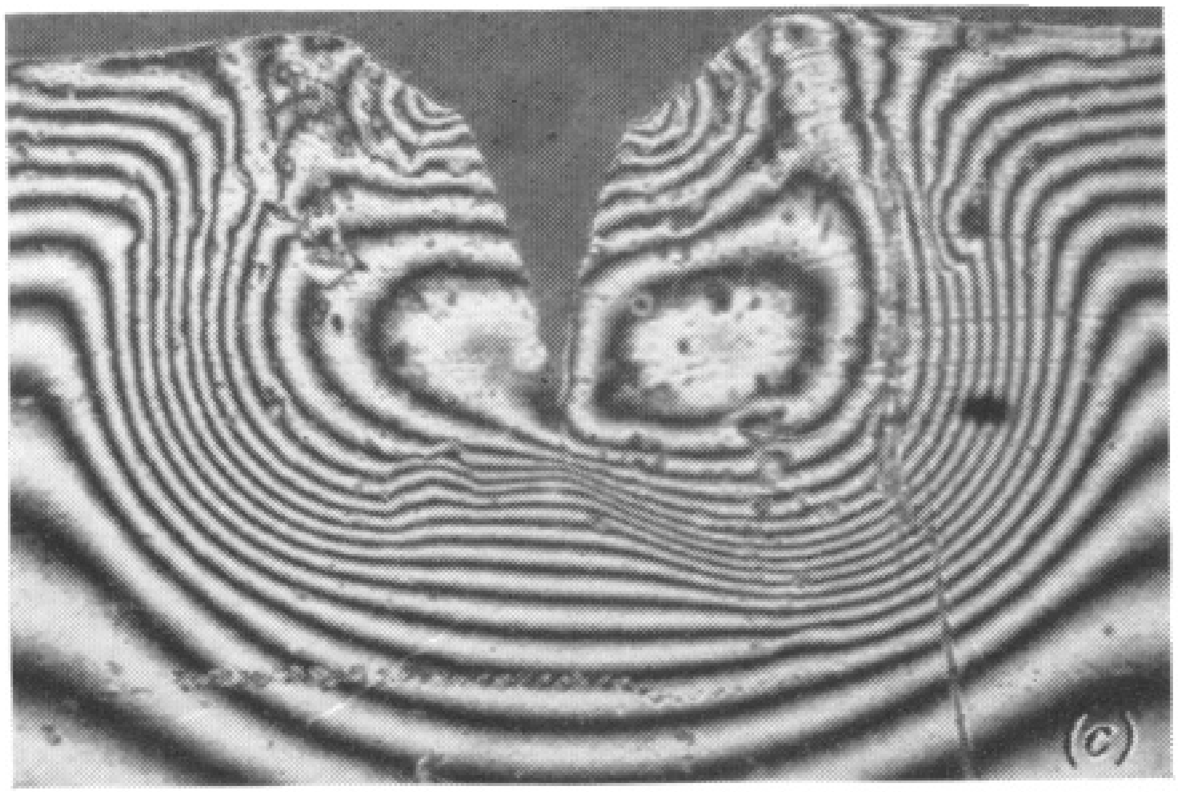

FIGURE 10. Subsurface deformation for Perspex. (Magn. $\times 140$.)
(a) 150° wedge indentation
(b) 120° wedge indentation
(c) 60° wedge indentation

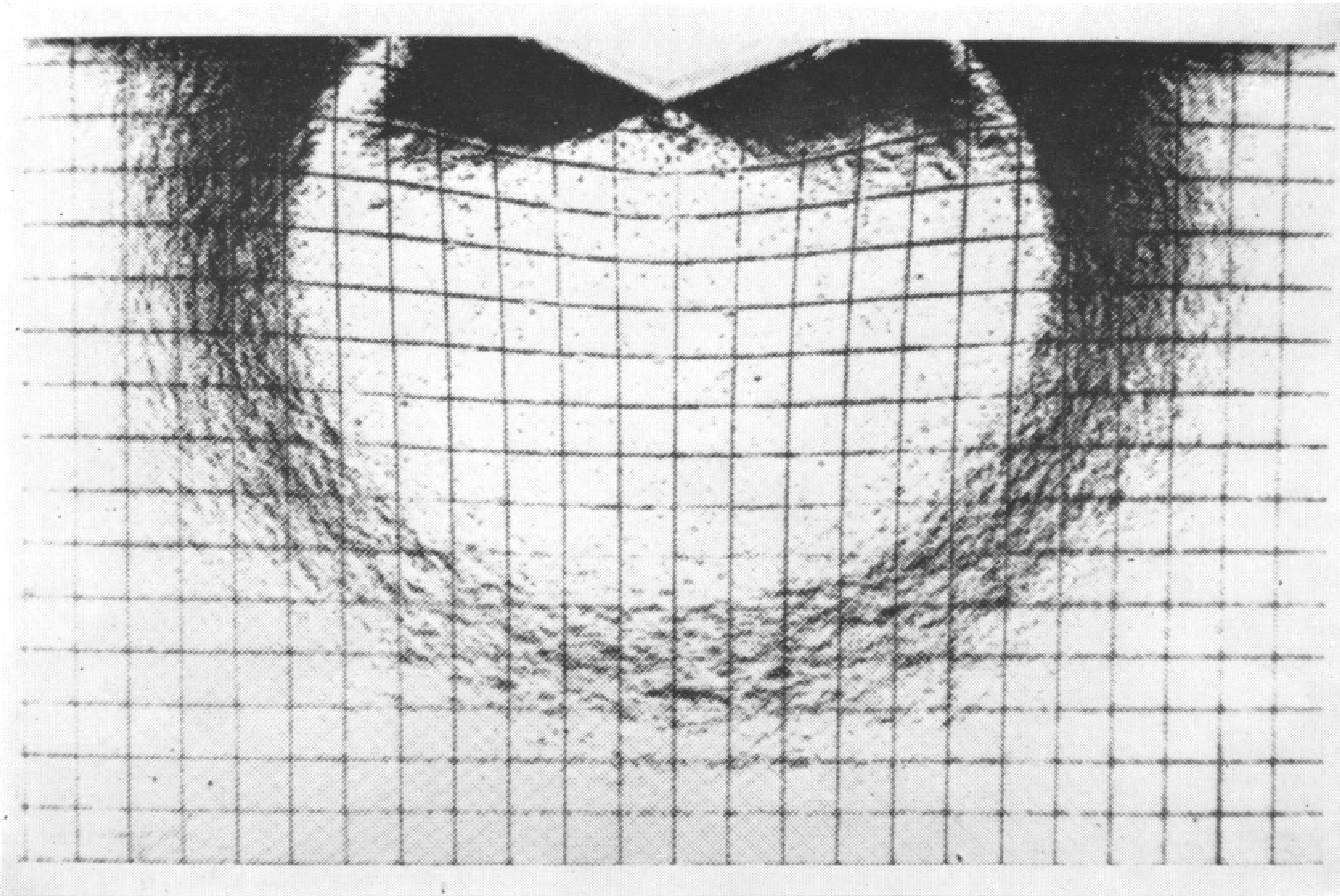

FIGURE 11. Deformation in radial compression (Mulhearn 1959).